Progress In Electromagnetics Research M, Vol. 118, 37–46, 2023

Optically Transparent Dual-Polarized Cross Dipole Antenna with Metal Mesh Film for 5G Applications

Haowei Xi[1], Xiaoliang Ge[2], Kuiwen Xu[1, *], Jianhua Shen[3], Xianglong Liu[2], and Xu Su[2]

Abstract—Optically transparent antennas have attracted increasing interest in recent years. However, the inherent ohmic loss of transparent conductor used in antennas will always introduce degradation of radiation efficiency. It is of most importance to find the optimization between the material loss and radiation efficiency. In this paper, we design and experimentally demonstrate a high-performance optically transparent dual-polarized cross dipole antenna over 3.4–3.8 GHz for 5G wireless communication based on the characteristic analysis of surface current distribution. By making current distribution uniform on the radiators and reducing the current on the ground, the mutual coupling between the elements is alleviated, and the radiation efficiency can be optimized. The proposed antenna is fabricated with 0.118-Ohm/sq meshed metal, and the optical transparency of antenna is 81%. The proposed antenna achieves a voltage standing wave ratio (VSWR) of less than 1.3, radiation efficiency of 72% (84% of pure copper), and a peak gain of 4.5 dBi (5.1 dBi of pure copper). Compared to current state-of-arts, the proposed antenna exhibits better performance of the figure of merit (FOM) in terms of the bandwidth, optical transparency, and radiation efficiency. Our work paves the way to diverse application of beyond-5G wireless communication.

1. INTRODUCTION

With the rapid development of wireless communication, antenna as an important RF component, its performance directly affects the quality of communication. As the spectrum of wireless communication continues to expand, and high-data transmission rate is demanded, the number of base stations in demand increases [1]. At present, limited number of 5G base stations are difficult to effectively cover both indoor and outside places, especially for the non-line-of-sight (NLOS) scenario with obstacles of buildings. A simple and efficient solution is to add more sub-stations and relay stations indoors to ensure the requirement of the high throughput communication [2]. Transparent antenna could be one of the main solutions in the next generation of indoor sub-station antenna, owing to its high transparency in visible frequency bands, soft visual impact, and being integrated flexibly with the glass in the building [3]. In the base-station antenna design, several characteristics such as wide bandwidth, dual polarization, and high radiation should be considered. However, these would bring some challenges via optical transparency.

At present, some transparent antennas have been proposed in the academical society. According to the used transparent materials, transparent antennas can be generally divided into two categories, the antennas printed on conductive film and some other nonplanar antennas with water [4, 5]. Printed antennas with some particular conductive film are widely concerned, such as the antennas based on AgHT films [6–8], F-doped Tin Oxide (FTO) films, and Indium Tin Oxide (ITO) [9–11]. However,

Received 24 May 2023, Accepted 10 July 2023, Scheduled 20 July 2023

* Corresponding author: Kuiwen Xu (kuiwenxu@hdu.edu.cn).

[1] Engineering Research Center of Smart Microsensors and Microsystems, Ministry of Education, Hangzhou Dianzi University, Hangzhou 310012, China. [2] State Key Laboratory of Integrated Optoelectronics, College of Electronic Science and Engineering, Jilin University, Changchun 130012, China. [3] The 54th Research Institute of CETC, Shijiazhuang 050081, China.

owing to the high sheet resistance of AgHT [7], the radiation efficiency is usually poor. ITO materials are preferable compared to AgHT materials, which have a high utilization rate in the design of ultra-wideband (UWB) transparent antenna [9], transparent reflection arrays [10], etc. [11]. However, both ITO and AgHT materials are fragile and expensive, which is one of the main obstacles to the widespread use of transparent antennas.

Recently, the metal mesh [12–16] with higher conductivity and lower sheet resistance has received intensive attention. Patch antenna fabricated in metal mesh materials is widely developed due to its simple design structure and flexible printed manufacture [13, 14]. However, they usually encounter relatively narrow bandwidth and low radiation efficiency due to large ohmic loss and physically large meta size. Therefore, transparent dipole antenna with less occupied area has relatively higher radiation efficiency [15]. In addition, metal mesh is also used to design transparent UWB Vivaldi antenna [16]. However, the performance in terms of radiation and optical transparency in above antennas is not satisfied. Usually, the realization of high-efficiency transparent antenna is at the expense of the transparency of the material, and the electrical conductivity is improved by using the material with low sheet resistance. Therefore, how to find an optimized-performance antenna within limited transparent conductors in a convenient way is highly required for antenna industries.

In this paper, a transparent antenna via meta-mesh films with dual-polarized cross dipole is proposed. The physical insight via surface current distribution is used for the characteristic analysis of the radiation performance. By properly modulating the current distribution on the radiators and reducing the amount of current distribution on the ground, the mutual coupling between the elements is alleviated, and the radiation efficiency of proposed antenna is significantly improved. Under the condition of sheet resistance of only $0.118\,\Omega$/sq and low-cost fabrication, measured results show that the dual-polarized antenna could achieve wide bandwidth of 3.4–3.8 GHz (5G band), with radiation efficiency of 72% (84% of pure copper) and the optical transparency of 81%. Compared to other state-of-art works, the proposed antenna has both higher optical transparency and better radiation performance, which can almost completely replace the pure copper antenna at some extent. Owing to being easily integrated with glass, it may have a wide range of applications and plays a significant role in promoting the development of 5G communications.

2. ANTENNA DESIGN

In this section, we would describe the principle of antenna design and discuss the insight analysis of the current distribution on the antenna performance. Finally, the optimal antenna structure and the corresponding parameters are determined.

2.1. Antenna Configuration

The configuration of the proposed optically transparent dual-polarized cross dipole antenna is shown in Fig. 1(b), as an improvement of Fig. 1(a), whose key parameters are depicted in Fig. 1(d). The proposed antenna is composed of a feeding coplanar waveguide (CPW), ground, and dual-polarized dipoles, as illustrated in Fig. 1(c). It incorporates three portions: dielectric substrate, radiation surface, and ground. Both the dipole and the ground are printed on the top of a dielectric substrate, which is constructed with metal mesh films. Its dielectric substrate is a piece of polyethylene terephthalate (PET) ($\varepsilon_r = 3$ and $\tan\delta = 0.002$) with a size of $188\,\text{mm} \times 184\,\text{mm} \times 1\,\text{mm}$. In order to make the antenna compact, the antenna uses two pairs of cross dipoles, which are designed to be positive and negative 45° vertically, to achieve $\pm 45^\circ$ dual line polarization. The whole dual-polarized antenna is symmetric about the Y-axis. The two arms of the dipole have different lengths and are used to produce the double resonances that forms wide bandwidth in the 5G frequency bands. A coplanar waveguide feeding structure is used to feed the antenna, and the two dipoles share the same middle ground. CPW has the characteristics of low dispersion and wide band, which is easy to connect with other components [19].

In order to exploit the radiation mechanism, the analysis of the current distribution is conducted via full-wave simulation. From the antenna theory, the radiation efficiency could be improved via decreasing the loss resistance R_L and the mutual coupling. Fig. 2(a) gives the detailed current distribution of the conventional antenna I. It can be seen that significant current distributes along the ground beside the

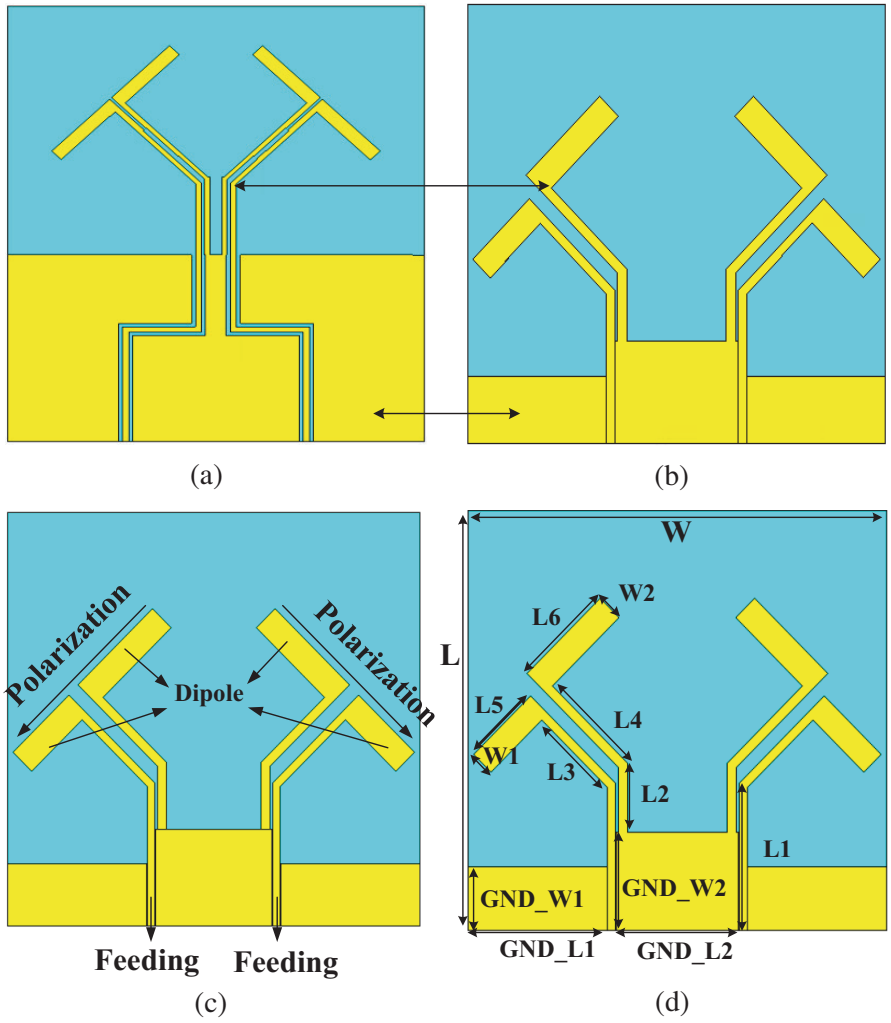

Figure 1. (a) Antenna I. (b) Antenna II. (c) Antenna Configuration. (d) Key parameters of the proposed antenna.

radiator, and the corresponding ohmic loss increases. There are also lots of surface current distributed on the arms of the other dipole, which means that strong coupling between the two dipoles also exists. Both of the aspects result in lower radiation efficiency. Therefore, to enhance the radiation efficiency, the distance between two dipoles is enlarged, and unaligned dipole is designed to improve the radiation resistance. Besides, the area of the ground is reduced greatly. According to the analysis of the current distribution from dual-polarized antenna, the ground of the CPW is redesigned as stepped structures to alleviate the intensity of the induced current on the ground. Through above operations, the mutual coupling between the dipoles from the air space and the common ground could also be reduced significantly. At the same time, the transparency of the antenna could be improved owing to the reduced area of the meta-mesh film.

As shown in Fig. 2(b), it can be seen that the coupling strength between the feeder and the ground is reduced, and most of the current density is along the edge of the excited.

Figure 3 depicts the simulated S-parameter and radiation efficiency versus different antenna structures I and II. Through these simulation results, it can be further verified that by optimizing the aforementioned key structures and reducing the mutual coupling, the antenna matches well, and the working bandwidth increases. At the same time, the radiation efficiency has been greatly improved.

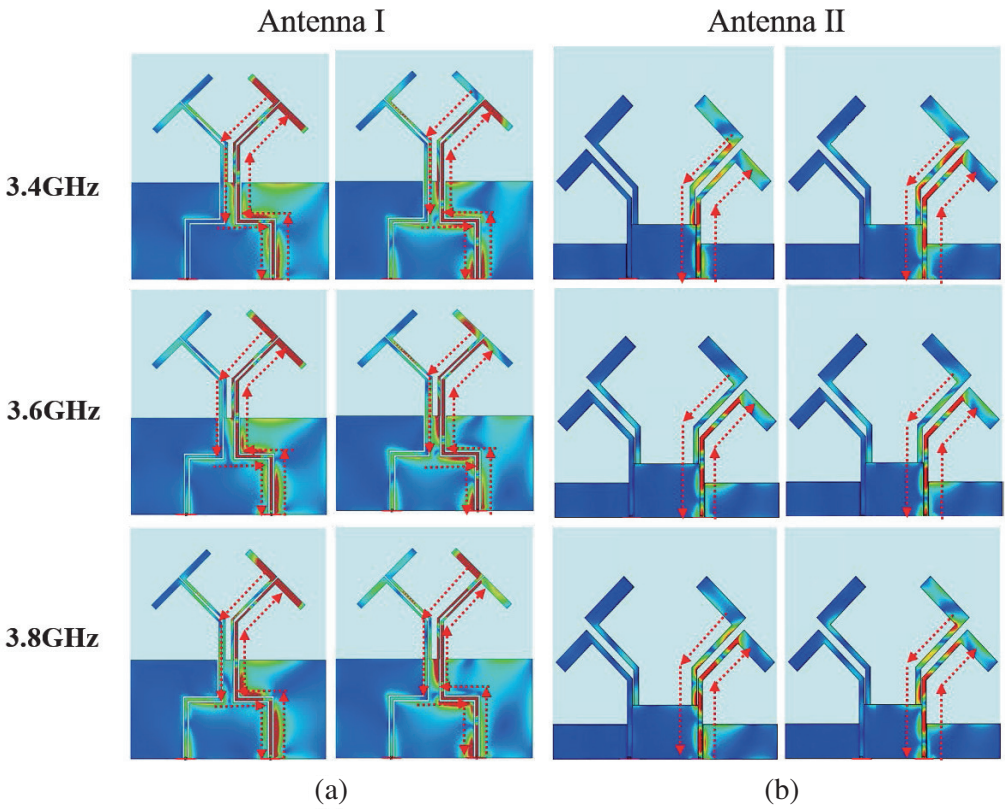

Figure 2. Current distribution diagram of antenna structures I and II.

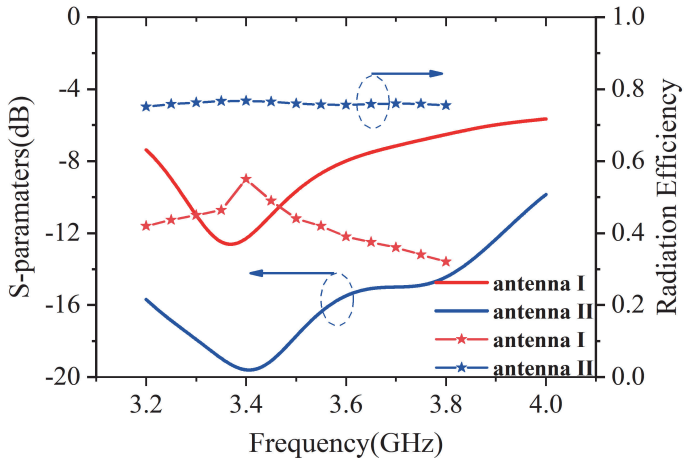

Figure 3. Simulation S-parameter and radiation efficiency versus different type of antenna.

2.2. Parametric Study

Based on the above physical analysis of the surface current, some parameters are optimized to achieve the best performance. Because the dual-polarization antennas are symmetric with the Y-axis, the influence of the parameter on the performance of the one antenna is studied.

The analysis of two arms of the dipole are shown in Figs. 4(a) and (b). With the increase of $L3$ length, the resonant frequency point gradually moves to the low frequency. Fig. 4(b) shows the length analysis of the right arm of the dipole. The radiation efficiency of low frequency increases with $L2$ being

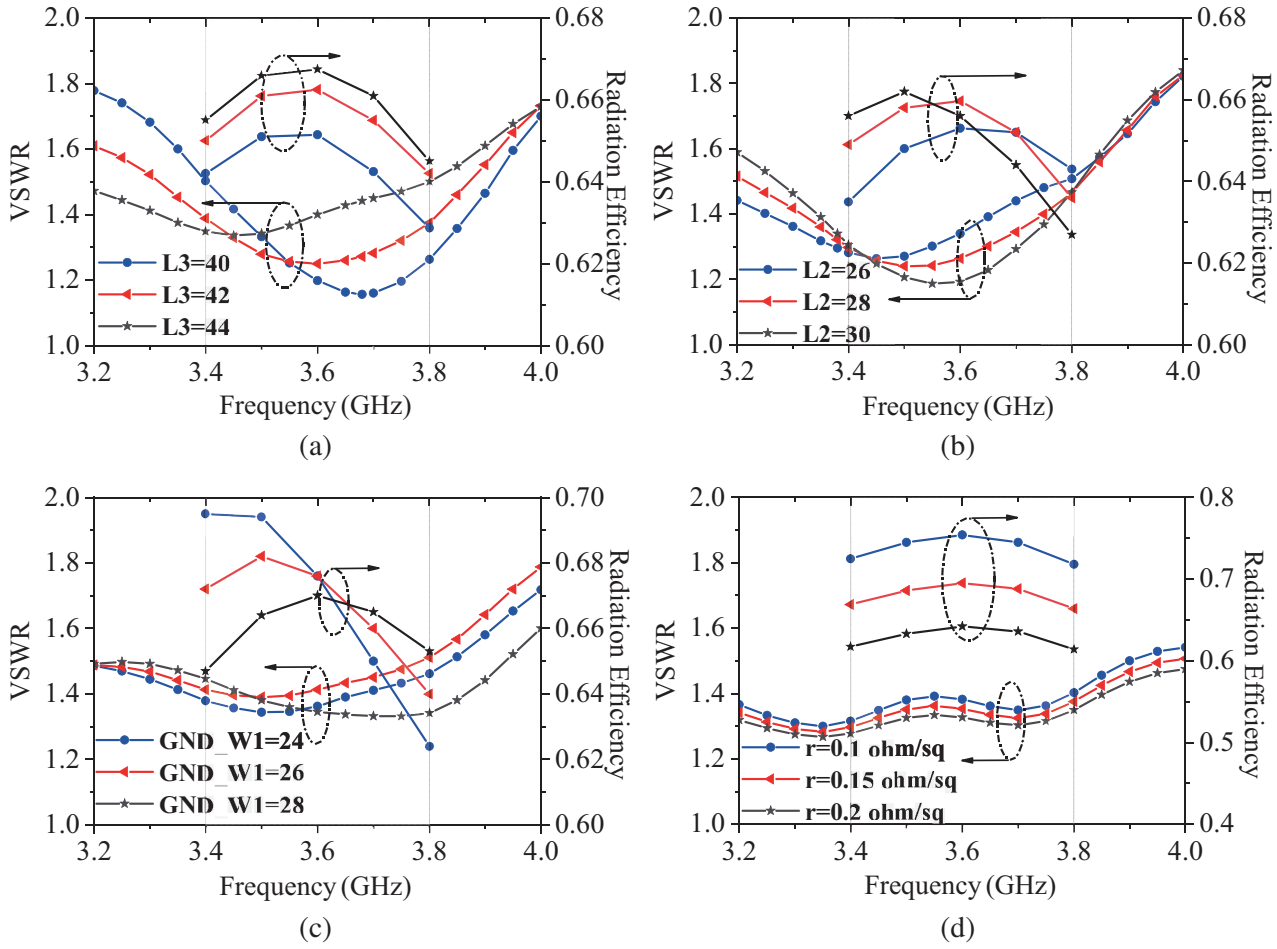

Figure 4. Key parameters analysis on the VSWR and radiation efficiency. (a) $L3$. (b) $L2$. (c) GND_$W1$. (d) Ohmic sheet resistance .

larger. When $L2$ increases to 28 mm, the high frequency radiation efficiency decreases. The results show that the overall radiation efficiency of the antenna can be adjusted by the two arms of the dipole. Fig. 4(c) shows the effect of width of the ground. As GND_$W1$ increases, the ground becomes larger, and the radiation efficiency of high frequency decreases while that of low frequency increases.

As shown in Fig. 4(d), the ohmic sheet of the meta-mesh films has little influence on the voltage standing wave ratio (VSWR) but a significant influence on the radiation efficiency. The smaller the ohmic sheet resistance is, the higher the radiation efficiency is. However, small sheet resistance would result in low transparency and high fabrication cost. A tradeoff should be kept by considering both radiation efficiency and optical transparency. Through the above optimization steps, the key structural parameters are determined to achieve the best performance. The optimized structural parameters are shown in Table 1.

Table 1. Characterizing parameter values of the antenna.

Parameters	L	W	$L1$	$L2$	$L3$	$L4$	$L5$	$L6$
Units(mm)	184	188	64.2	30	43.4	48	36	46.7
Parameters	W1	W2	GND_$L1$	GND_$L2$	GND_$W1$	GND_$W2$	CPW	GAP
Units(mm)	11	12	62.3	55	28	43	3.8	0.2

3. FABRICATION AND MEASUREMENT

The proposed antenna sample is fabricated with the use of a photolithography-assisted nano-imprinting technology. Antenna prototype is composed of pure copper and transparent materials, respectively, as shown in Figs. 5(a) and (b). Both the proposed transparent antenna and opaque antenna (e.g., pure copper) are measured by vector network analyzer and microwave anechoic chamber to verify the feasibility of the design.

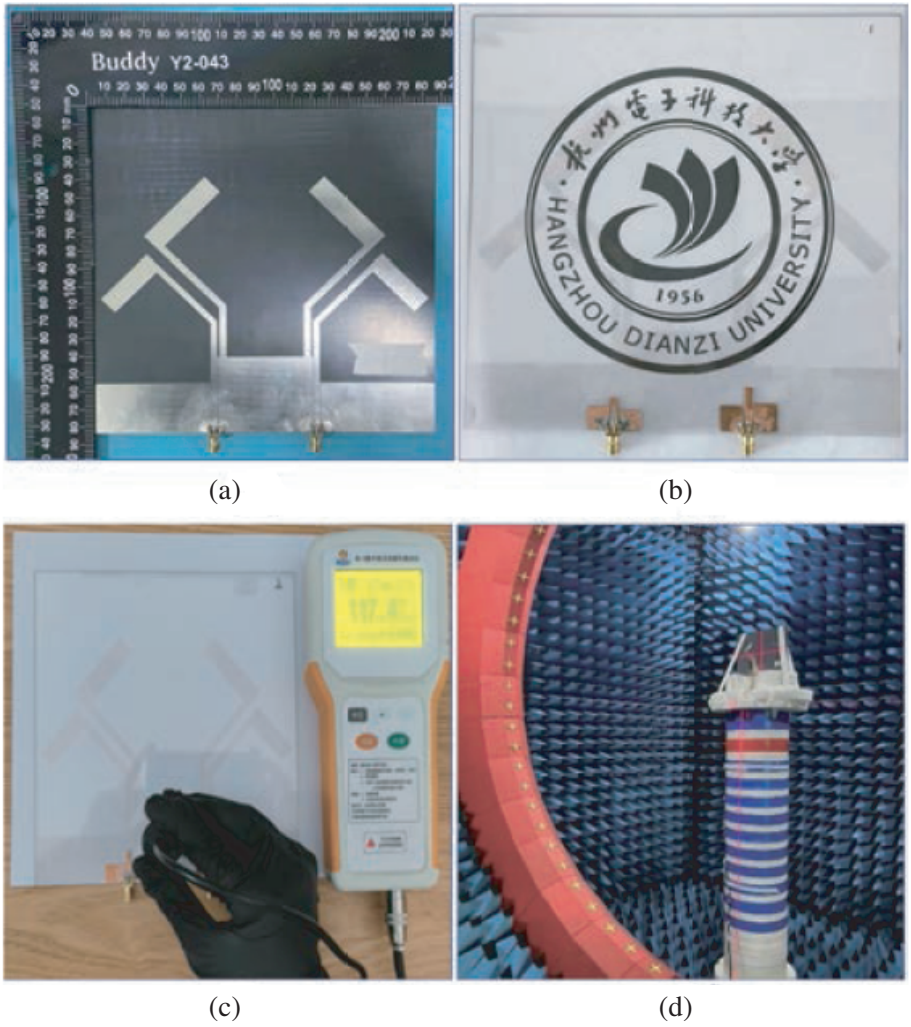

Figure 5. Fabricated antenna, (a) copper antenna, (b) transparent antenna, (c) measured sheet resistance, (d) measurement environment.

In order to accurately measure the ohmic sheet resistance of transparent materials, a sheet resistance meter is used to test the sheet resistance of transparent antenna, as shown in Fig. 5. The measured values are the average of 10 points randomly distributed on the surface of the transparent antenna. The final measured sheet resistance is about 0.118 Ω/sq.

The simulated and measured VSWRs and S-parameters S_{21} of transparent antenna and opaque antenna are shown in Fig. 6. It can be seen from Fig. 6 that antennas are well matched. The VSWR of the proposed transparent antenna is lower than 1.4 in the operating frequency band, i.e., 3.4–3.8 GHz, in which relative bandwidth is about 21.8% and is wider than the simulation 12.3%. Besides, the isolation of the dual-polarization antennas is quite good, and the measured S_{21} is lower than −20 dB. All the measured S-parameters show good agreement with the simulated results.

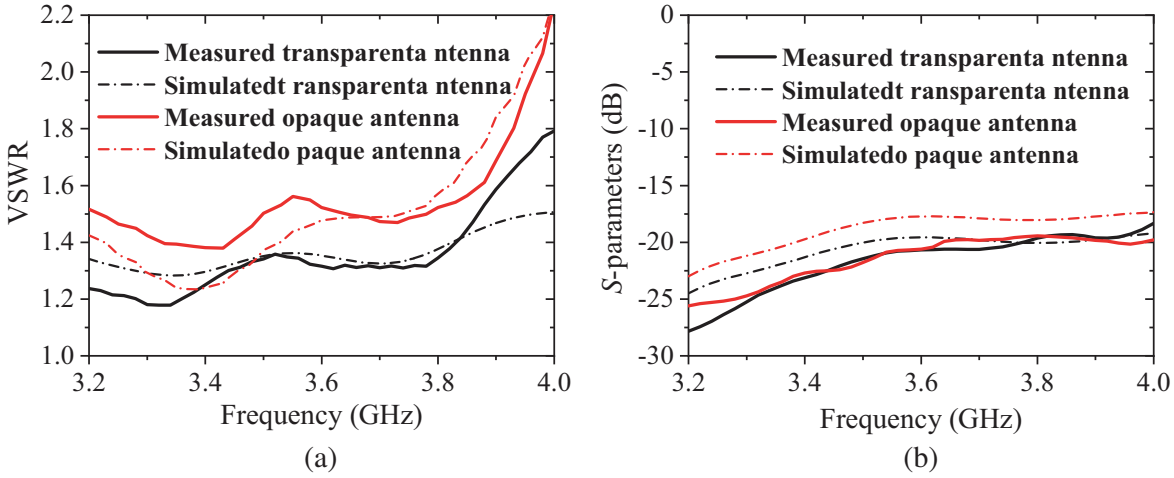

Figure 6. Measurement and simulation results of S-parameter. (a) VSWR. (b) S-parameter S_{21}.

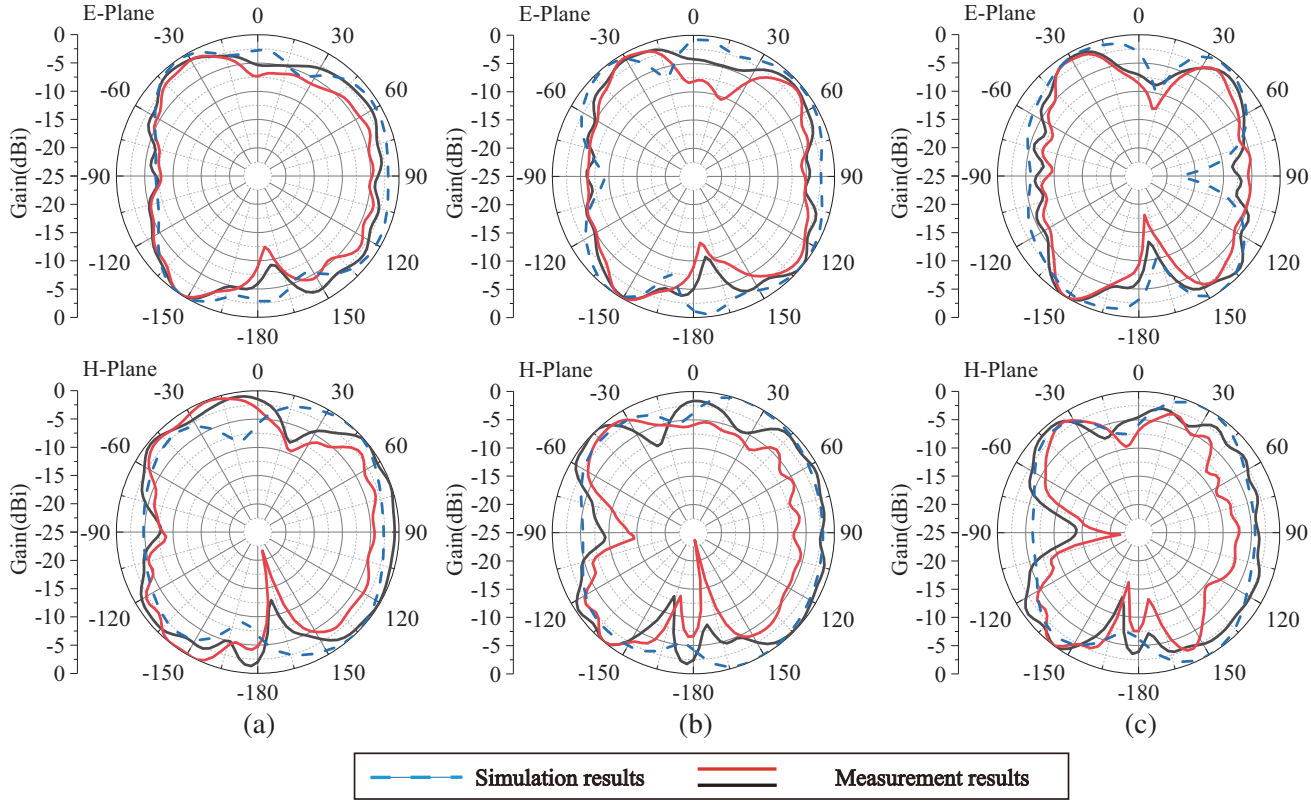

Figure 7. Simulation and measured radiation pattern different frequencies. (a) 3.4 GHz, (b) 3.6 GHz and (c) 3.8 GHz.

The radiation patterns of the proposed antenna and opaque antenna are depicted in Fig. 7. As can be seen from the measured results, the proposed antenna exhibits good omnidirectional and stable radiation patterns in the operating frequency band of 3.4–3.8 GHz. The peak gains of the opaque antenna and transparent antenna are 5.1 dBi and 4.5 dBi, respectively. As depicted in Fig. 8, the realized gain keeps stable in the whole operating band, and the average gain is about 4 dBi. Compared with the simulated results, the measured gain of the transparent antenna is a little lower than that of

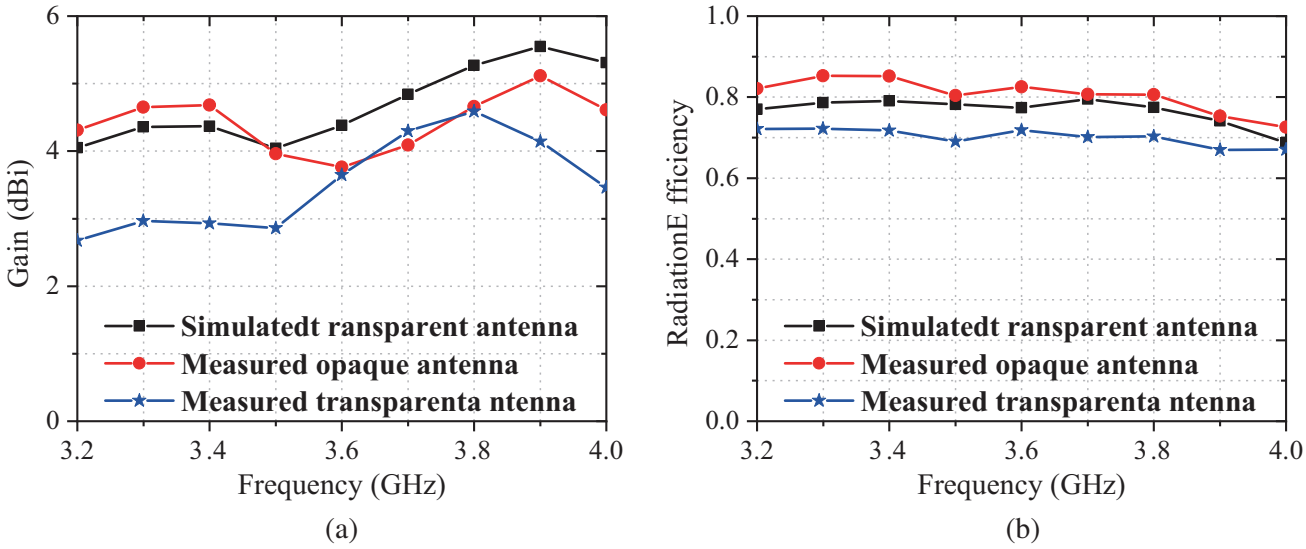

Figure 8. Measured and simulated results of gain and efficiency. (a) Gain. (b) Radiation efficiency.

simulation. The maximum measured gain and simulated one of transparent antenna are about 4.5 dBi and 5.5 dBi, respectively. Besides, the radiation efficiency of the proposed transparent antenna reaches 72%, which is reduced by about 10% compared to the opaque antenna (e.g., pure copper). Therefore, there are some deviations between the measured and simulated ones, which is probably owing to the loss of the fabricated metal mesh and the connected cables.

The comparisons with other transparent antennas reported recently are listed in Table 2. Our work has two distinct advances. Firstly, mesh metal has better performance in terms of the low sheet resistance, high transparency, easy fabrication and integration. Secondly, by use of characteristic analysis and optimization of current distribution, the influence of ohmic loss on the radiation efficiency is significantly alleviated, and the proposed antenna has the best performance of the figure of merit (FOM) in terms of the operating band, radiation efficiency, and optical transparency with a higher sheet resistance of the meta-mesh film.

Table 2. Comparison between various transparent antennas.

Ref.	Material	Antenna	BW%	Max Gain	OT%	Fom	Sheet Resistance
[4]	Pure Water	Dipole	4.08%	3.2 dB	72%	1.38%	0.1 Ω/sq
[5]	Salt Water	Dipole	1.3%	2.0 dB	96%	9.38%	N.A.
[8]	AgHT	Patch	4.26%	2.4 dB	N.A.	N.A.	0 Ω/sq
[13]	Meshed metal	Patch	N.A.	4.14 dB	82.64%	N.A.	N.A.
[14]	Meshed metal	Patch	N.A.	2.63 dB	60%	N.A.	0.18 Ω/sq
[15]	Meshed metal	Dipole	18.18%	2.4 dB	70%	7.13%	0.04 Ω/sq
[17]	Grid wires	Patch	10.53%	1.73 dB	90%	4.14%	N.A.
[18]	AgGL	Slot	3%	5 dB	70.7%	1.27%	0.05 Ω/sq
This work	Meshed metal	Dipole	21.8%	4.5 dB	81%	12.55%	0.118 Ω/sq

* Q% Q=BW%*OT%*ave_Efficiency% (Quality factor).
* BW% refers to the impedance bandwidth with ($S_{11} < -15$ dB).
* OT% refers to the optical transparency and N.A. refers to not available

4. CONCLUSION

An optically transparent dual-polarized cross dipole antenna with metal mesh is proposed for 5G wireless communication. The physical insight and analysis via surface current distribution is used for the characteristic analysis of the radiation performance. By properly modulating the current distribution on the radiators and reducing the area of the current distribution on the ground, the mutual coupling between the radiators and the loss owing to the sheet resistance is alleviated, and the radiation efficiency of proposed antenna is also accordingly improved. From the overall measurement results, the proposed antenna has a wide bandwidth of 3.4–3.8 GHz (5G band) and stable radiation pattern in the working frequency band. The maximum radiation efficiency of transparent antenna is 72%, and the optical transparency reaches 81% with the sheet resistance as low as 0.118 Ω/sq. In the future, the proposed antenna could be taken as the elements to construct the antenna array on the conformal surfaces to generate the required far-field radiation patterns [20]. In the future era of internet of things and 5G, transparent antenna would have broader application scenarios in the wireless communication.

ACKNOWLEDGMENT

This work was supported in part by the National Natural Science Foundation of China under Grant No. 62293493, Grant No. 61971174.

REFERENCES

1. Lindmark, B. and M. Nilsson, "On the available diversity gain from different dual-polarized antennas," *IEEE Journal on Selected Areas in Communications*, Vol. 19, No. 2, 287–294, 2001.
2. Lee, S. and K. Huang, "Coverage and economy of cellular networks with many base stations," *IEEE Antennas Wireless Propag. Lett.*, Vol. 16, No. 7, 1038–1040, 2012.
3. Lu, X., Y. Chen, S. Guo, and S. Yang, "An electromagnetic-transparent cascade comb dipole antenna for multi-band shared-aperture base station antenna array," *IEEE Trans. Antennas Propag.*, Vol. 70, No. 4, 2750–2759, 2022.
4. Sayem, A. S. M., R. B. V. B. Simorangkir, K. P. Esselle, R. M. Hashmi, and H. Liu, "A method to develop flexible robust optically transparent unidirectional antennas utilizing pure water, PDMS, and transparent conductive Mesh," *IEEE Trans. Antennas Propag.*, Vol. 68, No. 10, 6943–6952, 2020.
5. Duy Tung, P. and C. W. Jung, "Highly transparent planar dipole using liquid ionized salt water under surface tension condition for UHD tv applications," *IEEE Trans. Antennas Propag.*, Vol. 69, No. 1, 35–42, 2021.
6. Malek, M. A., S. Hakimi, S. K. Abdul Rahim, and A. K. Evizal, "Dual-band CPW-fed transparent antenna for active RFID tags," *IEEE Antennas Wireless Propag. Lett.*, Vol. 14, 919–922, 2015.
7. Peter, T., R. Nilavalan, H. F. Abu Tarboush, and S. W. Cheung, "A novel technique and soldering method to improve performance of transparent polymer antennas," *IEEE Antennas Wireless Propag. Lett.*, Vol. 9, 918–921, 2010.
8. Song, H. J., T. Y. Hsu, D. F. Sievenpiper, H. P. Hsu, J. Schaffner, and E. Yasan, "A method for improving the efficiency of transparent film antennas," *IEEE Antennas Wireless Propag. Lett.*, Vol. 7, 753–756, 2008.
9. Potti, D. and Y. Tusharika, "A novel optically transparent UWB antenna for automotive MIMO communications," *IEEE Trans. Antennas Propag.*, Vol. 69, No. 7, 3821–3828, 2021.
10. Kocia, C. and S. V. Hum, "Design of an optically transparent reflectarray for solar applications using indium tin oxide," *IEEE Trans. Antennas Propag.*, Vol. 64, No. 7, 2884–2893, 2016.
11. Haraty, M. R., M. Naser-Moghadasi, A. A. Lotfi-Neyestanak, and A. Nikfarjam, "Improving the efficiency of transparent antenna using gold nanolayer deposition," *IEEE Antennas Wireless Propag. Lett.*, Vol. 15, 4–7, 2016.

12. Ding, C., L. Liu, and K.-M. Luk, "An optically transparent dual-polarized stacked patch antenna with metal-mesh films," *IEEE Antennas Wireless Propag. Lett.*, Vol. 18, No. 10, 1981–1985, 2019.
13. Kang, S. H. and C. W. Jung, "Transparent patch antenna using metal mesh," *IEEE Trans. Antennas Propag.*, Vol. 66, No. 4, 2095–2100, 2018.
14. Hong, S., Y. Kim, and C. Won Jung, "Transparent microstrip patch antennas with multilayer and metal-mesh films," *IEEE Antennas Wireless Propag. Lett.*, Vol. 16, 772–775, 2017.
15. Duy Tung, P. and C. W. Jung, "Optically transparent wideband dipole and patch external antennas using metal mesh for UHD tv applications," *IEEE Trans. Antennas Propag.*, Vol. 68, No. 3, 1907–1917, 2020.
16. Wu, B., X.-Y. Sun, H.-R. Zu, H.-H. Zhang, and T. Su, "Transparent ultra-wideband halved coplanar Vivaldi antenna with metal mesh film," *IEEE Antennas Wireless Propag. Lett.*, Vol. 21, No. 12, 2532–2536, 2022.
17. Hong, W., S. Lim, S. Ko, and Y. G. Kim, "Optically invisible antenna integrated within an OLED touch display panel for IoT applications," *IEEE Trans. Antennas Propag.*, Vol. 69, No. 5, 2853–2863, 2021.
18. Hautcoeur, J., F. Colombel, M. Himdi, X. Castel, and E. M. Cruz, "Large and optically transparent multilayer for broadband H-shaped slot antenna," *IEEE Antennas Wireless Propag. Lett.*, Vol. 12, 933–936, 2013.
19. Jackson, R. W., "Considerations in the use of coplanar waveguide for millimeter-wave integrated circuits," *IEEE Trans. Microw. Theory Tech.*, Vol. 34, No. 12, 1450–1456, 1986.
20. Morabito, A. F., R. Palmeri, V. A. Morabito, A. R. Lagana', and T. Isernia, "Single-surface phaseless characterization of antennas via hierarchically ordered optimizations," *IEEE Trans. Antennas Propag.*, Vol. 67, No. 1, 461–474, Jan. 2019.